Polyhedron 117 (2016) 367–376

Contents lists available at ScienceDirect

Polyhedron

journal homepage: www.elsevier.com/locate/poly

Synthesis, spectroscopic and X-ray characterization of various pyrazine-bridged platinum(II) complexes: ^{1}H NMR comparative study of their catalytic abilities in the hydrolysis of methionine- and histidine-containing dipeptides

Snežana Rajković [a], Marija D. Živković [a], Beata Warżajtis [b], Urszula Rychlewska [b,*], Miloš I. Djuran [a,*]

[a] Department of Chemistry, Faculty of Science, University of Kragujevac, R. Domanovića 12, 34000 Kragujevac, Serbia
[b] Faculty of Chemistry, Adam Mickiewicz University, Umultowska 89^B, 61-614 Poznań, Poland

ARTICLE INFO

Article history:
Received 14 March 2016
Accepted 8 June 2016
Available online 15 June 2016

Keywords:
Pyrazine-bridged platinum(II) complex
X-ray crystallography
Methionine- and histidine-containing dipeptides
NMR spectroscopy
Hydrolysis

ABSTRACT

Four pyrazine (pz)-bridged Pt(II) complexes, [{Pt(1,3-pd)Cl}$_2$(μ-pz)]Cl$_2$·LiCl (**1**) (1,3-pd = 1,3-propylenediamine), [{Pt(2,2-diMe-1,3-pd)Cl}$_2$(μ-pz)]Cl$_2$·2[Li(H$_2$O)$_4$]Cl·2H$_2$O (**2**) (2,2-diMe-1,3-pd = 2,2-dimethyl-1,3-propylenediamine), [{Pt(1,3-pnd)Cl}$_2$(μ-pz)](ClO$_4$)$_2$·H$_2$O (**3**) (1,3-pnd = (±)-1,3-pentanediamine) and [{Pt(1,3-pnd)Cl}$_2$(μ-pz)]Cl$_2$·2[Pt(1,3-pnd)Cl$_2$]·2H$_2$O (**4**) have been synthesized. NMR and UV–Vis spectroscopic characterization has been performed for compounds **1**–**3**, while single-crystal X-ray analysis has been carried out for complexes **2** and **4**. Atomic distribution in the crystals of **4** indicated a disorder which could be attributed to the presence at the same crystallographic site of four distinct stereoisomers of the [{Pt(1,3-pnd)Cl}$_2$(μ-pz)]$^{2+}$ complex cation. The presence of four stereoisomeric products was also observed in complex **3** by ^{13}C NMR spectroscopy. Complexes **1**–**3** were converted into the corresponding aqua complexes, [{Pt(X)(H$_2$O)}$_2$(μ-pz)]$^{4+}$ (X is 1,3-pd, 2,2-diMe-1,3-pd and 1,3-pnd, respectively), and ^{1}H NMR spectroscopy was applied for comparison of their catalytic activities with those of the analogous mononuclear [Pt(X)(H$_2$O)$_2$]$^{2+}$ and pyrazine-bridged [{Pt(en)(H$_2$O)}$_2$(μ-pz)]$^{4+}$ complexes in the hydrolysis of the *N*-acetylated L-methionylglycine (Ac-L-Met-Gly) and L-histidylglycine (Ac-L-His-Gly). All reactions were performed in the pH range 2.0–2.5 at 37 °C. It was found that all investigated dinuclear Pt(II)-aqua complexes promote selective cleavage of the amide bond involving carboxylic group of the anchoring amino acid methionine in the Ac-L-Met-Gly or histidine in the Ac-L-His-Gly. ^{1}H NMR data indicate that neither the size of the chelated diamine ring (five-membered in ethylenediamine and six-membered in 1,3-propylenediamine) nor the bulky substituents incorporated into the 1,3-propylenediamine ligand have significant influence on the rate of hydrolysis of Ac-L-Met-Gly dipeptide. Meanwhile, the rate of hydrolysis of Ac-L-His-Gly depends on both of these factors and decreases in order en > 1,3-pd > 1,3-pnd > 2,2-diMe-1,3-pd. Moreover, it has been shown that all investigated dinuclear Pt(II)-aqua complexes are better catalytic agents in the hydrolysis of the dipeptides than the analogous mononuclear Pt(II)-aqua complexes. The present findings are expected to play a crucial role in the development of new Pt(II) complexes, which can act as effective catalytic reagents for the selective hydrolysis of peptides containing either methionine or histidine residues.

1. Introduction

Our recent interest in the study of the reactions between dinuclear platinum(II) complexes with bridging diazine ligands and methionine- and histidine-containing peptides stems from the findings that these complexes can be an effective catalytic reagents for the regioselective amide bond hydrolysis in these peptides [1–3]. In accordance to this, the ^{1}H NMR study of the hydrolytic reactions between two Pt(II) complexes, mononuclear [Pt(en)(H$_2$O)$_2$]$^{2+}$ (en is ethylenediamine) and dinuclear [{Pt(en)(H$_2$O)}$_2$(μ-pz)]$^{4+}$ (pz is pyrazine), and *N*-acetylated L-methionylglycine (Ac-L-Met-Gly) have shown that in comparison with the mononuclear Pt(II) complex, the two Pt(II) ions bridged with one aromatic pyrazine ligand in the [{Pt(en)(H$_2$O)}$_2$(μ-pz)]$^{4+}$ complex are more efficient in the hydrolysis of the Ac-L-Met-Gly dipeptide,

* Corresponding authors. Fax: +48 61 829 1555 (U. Rychlewska), +381 34 335040 (M.I. Djuran).
E-mail addresses: urszular@amu.edu.pl (U. Rychlewska), djuran@kg.ac.rs (M.I. Djuran).

http://dx.doi.org/10.1016/j.poly.2016.06.011
0277-5387/

even when the hydrolytic reaction was performed with an excess of $[Pt(en)(H_2O)_2]^{2+}$ complex [1]. Moreover, reactions of two dinuclear diazine-bridged Pt(II) aqua complexes, $[\{Pt(en)(H_2O)\}_2(\mu\text{-pz})]^{4+}$ and $[\{Pt(en)(H_2O)\}_2(\mu\text{-pydz})]^{4+}$ (pydz is pyridazine), with Ac-L-Met-Gly and Ac-L-His-Gly indicated that the $[\{Pt(en)(H_2O)\}_2(\mu\text{-pydz})]^{4+}$ complex reacts only with methionine sulfur atom and promotes the sole cleavage of the amide bond involving the carboxylic group of this anchoring amino acid, while the analogous pyrazine Pt(II) aqua dimer reacts with both residues, promoting cleavage of the amide bonds involving the carboxylic groups of both amino acids, methionine and histidine [2]. The catalytic disparity of these two diazine-bridged Pt(II) aqua dimers was explained by the X-ray analysis of their chlorido analogues, $[\{Pt(en)Cl\}_2(\mu\text{-pydz})]Cl_2$ and $[\{Pt(en)Cl\}_2(\mu\text{-pz})]Cl_2$. The X-ray data for the two complexes confirmed the presence of a hidden position of the Pt(II) centers in the $[\{Pt(en)Cl\}_2(\mu\text{-pydz})]Cl_2$ complex caused by their close proximity due to the *ortho*-substitution (the two Pt(II) centers are only 3.2535(4) Å apart), compared to the separation of 6.7890(3) Å in $[\{Pt(en)Cl\}_2(\mu\text{-pz})]Cl_2$), and an additional steric hindrance from the amine ligand, which in $[\{Pt(en)Cl\}_2(\mu\text{-pydz})]Cl_2$ is hydrogen bonded to the chlorido ligand belonging to the other Pt(II) center. Also, it was proposed that displacement of this chlorido ligand by a water molecule would make this hydrogen bond shorter due to the shortening of the metal–ligand bond distance [2].

In the course of the above investigations, we have recently studied the rate of hydrolysis of the amide bond in Ac-L-Met-Gly dipeptide in the presence of various $[\{Pt(X)(H_2O)\}_2(\mu\text{-pz})]^{4+}$ type complexes (X stands for bidentate coordinated diamine ligands ethylenediamine, en; (±)-1,2-propylenediamine, 1,2-pn; isobutylenediamine, ibn; *trans*-(±)-1,2-diaminocyclohexane, dach) [3]. We have demonstrated that the hydrolytic cleavage of the amide bond involving the carboxylic group of methionine in Ac-L-Met-Gly dipeptide decreases in order en > 1,2-pn > ibn > dach, hence can be notably hindered by increasing steric crowding in the diamine part of the $[\{Pt(X)(H_2O)\}_2(\mu\text{-pz})]^{4+}$ complex. Giving importance to the fact that dinuclear Pt(II) complexes with diazine-bridged ligands were shown to be effective catalytic reagents for the hydrolytic cleavage of the amide bonds in the methionine- and histidine-containing peptides and that selectivity and efficiency of this hydrolytic reaction could be controlled by structural modification of these dinuclear Pt(II) complexes, we have synthesized four pyrazine (pz)-bridged Pt(II) complexes, $[\{Pt(1,3\text{-pd})Cl\}_2(\mu\text{-pz})]Cl_2\cdot LiCl$ (**1**) (1,3-pd = 1,3-propylenediamine), $[\{Pt(2,2\text{-diMe-}1,3\text{-pd})Cl\}_2(\mu\text{-pz})]Cl_2\cdot 2[Li(H_2O)_4]Cl\cdot 2H_2O$ (**2**) (2,2-diMe-1,3-pd = 2,2-dimethyl-1,3-propylenediamine), $[\{Pt(1,3\text{-pnd})Cl\}_2(\mu\text{-pz})](ClO_4)_2\cdot H_2O$ (**3**) (1,3-pnd = (±)-1,3-pentanediamine) and $[\{Pt(1,3\text{-pnd})Cl\}_2(\mu\text{-pz})]Cl_2\cdot 2[Pt(1,3\text{-pnd})Cl_2]\cdot 2H_2O$ (**4**). Compounds **1**–**3** were characterized by elemental microanalysis, NMR and UV–Vis spectroscopy. The structures of dinuclear complexes **2** and **4** have been established by single-crystal X-ray diffraction analysis. The catalytic activities of the aqua derivatives of **1**–**3**, with general formulae $[\{Pt(X)(H_2O)\}_2(\mu\text{-pz})]^{4+}$ (X is 1,3-pd, 2,2-diMe-1,3-pd and 1,3-pnd, respectively), in the reactions with Ac-L-Met-Gly and Ac-L-His-Gly dipeptides have been investigated by applying ^1H NMR spectroscopy.

2. Experimental

2.1. Materials

Distilled water was demineralized and purified to a resistance greater than 10 MΩ cm^{-1}. The compounds D_2O, DNO_3, NaOD, 1,3-propylenediamine (1,3-pd), (±)-1,3-pentanediamine (1,3-pnd), 2,2-dimethyl-1,3-propylenediamine (2,2-diMe-1,3-pd), pyrazine (pz) and $K_2[PtCl_4]$ were purchased from the Sigma–Aldrich Chemical Co. All common chemicals were of reagent grade. The dipeptides L-Met-Gly and L-His-Gly were obtained from Bachem A.G. The terminal amino group in these peptides was acetylated by a standard method [4]. The mononuclear platinum(II) complexes of the type $[Pt(X)Cl_2]$ (X is 1,3-pd, 2,2-diMe-1,3-pd and 1,3-pnd) were synthesized according to a procedure published in the literature [5–7]. $K_2[PtCl_4]$ was dissolved in water and mixed with an equimolar amount of diamine ligand. The pH of the solution was adjusted to ca. 3 by addition of 1 M HCl and the mixture was stirred at 80 °C for 2 h. All complexes were crystallized from water at room temperature. The pure complexes were obtained by recrystallization from a small amount of water. The yield was between 80–90%. These complexes were used for further synthesis of the corresponding pyrazine-bridged Pt(II) complexes.

2.2. Synthesis of Pt(II) dinuclear complexes *1*–*4*

The complexes $[\{Pt(1,3\text{-pd})Cl\}_2(\mu\text{-pz})]Cl_2\cdot LiCl$ (**1**), $[\{Pt(2,2\text{-diMe-}1,3\text{-pd})Cl\}_2(\mu\text{-pz})]Cl_2\cdot 2[Li(H_2O)_4]Cl\cdot 2H_2O$ (**2**), $[\{Pt(1,3\text{-pnd})Cl\}_2(\mu\text{-pz})](ClO_4)_2\cdot H_2O$ (**3**) and $[\{Pt(1,3\text{-pnd})Cl\}_2(\mu\text{-pz})]Cl_2\cdot 2[Pt(1,3\text{-pnd})Cl_2]\cdot 2H_2O$ (**4**) were synthesized by modification of the procedure published in the literature [1,8,9].

The mononuclear $[Pt(X)Cl_2]$ complex was converted into the corresponding monodimethylformamide (dmf) complex $[Pt(X)Cl(dmf)]NO_3$ by treatment with 0.98 equivalents of $AgNO_3$. To a solution of 55.3 mg (0.325 mmol) of $AgNO_3$ in 5 cm^3 of dmf was added a suspension of 0.332 mmol of $[Pt(X)Cl_2]$ in 10 cm^3 of dmf. The mixture was stirred overnight at room temperature in the dark. The precipitated AgCl was removed by filtration and the resulting pale yellow dmf solution of $[Pt(X)Cl(dmf)]NO_3$ was used as a starting material for the preparation of the required pyrazine-bridged platinum(II) complexes.

The dmf solution of the pyrazine ligand (13.29 mg, 0.166 mmol) was added dropwise to the solution of $[Pt(X)Cl(dmf)]NO_3$. The mixture was stirred at room temperature in the dark for 12 h. The solvent was then rotary evaporated and the residue washed with ether. The crude product was dissolved in a minimal amount of 0.5 mol/dm^3 LiCl aqueous solution for **1**, **2** and **4** or 0.5 mol/dm^3 $LiClO_4$ for **3**. The obtained solution was left overnight in the dark. The pale-yellow precipitate of the corresponding dinuclear Pt(II) complex was removed by filtration, washed with methanol and then ether, and air-dried. Depending on the type of diamine ligand (X) the yield of complexes **1**–**4** was between 35% and 40%. *Anal.* Calc. for **1** = $C_{10}H_{24}Cl_5LiN_6Pt_2$ (FW = 802.70): C, 14.96; H, 3.01; N, 10.47. Found: C, 14.80; H, 3.03; N, 10.07%. *Anal.* Calc. for **2** = $C_{14}H_{52}Cl_6Li_2N_6O_{10}Pt_2$ (FW = 1081.35): C, 15.55; H, 4.85; N, 7.77. Found: C, 16.04; H, 4.72; N, 8.17%. *Anal.* Calc. for **3** = $C_{14}H_{34}Cl_4N_6O_9Pt_2$ (FW = 962.43): C, 17.47; H, 3.56; N, 8.73. Found: C, 17.46; H, 3.48; N, 8.58%. *Anal.* Calc. for **4** = $C_{24}H_{64}Cl_8N_{10}O_2Pt_4$ (FW = 1588.77): C, 18.14; H, 4.06; N, 8.82. Found: C, 18.16; H, 3.80; N, 8.84%.

2.3. Preparation of aqua Pt(II) complexes

The dinuclear chlorido complexes **1**–**3** were converted into the corresponding aqua derivatives, with general formulae $[\{Pt(X)(H_2O)\}_2(\mu\text{-pz})]^{4+}$, according to a previously published method [10] by treatment with 4.98, 5.98 and 3.98 equivalents of $AgNO_3$ for **1**–**3**, respectively. The same method was used for the preparation of mononuclear $[Pt(X)(H_2O)_2]^{2+}$ complexes starting from the corresponding chlorido complexes by reacting with $AgNO_3$ in 1:1.98 molar ratio, respectively. In each case, the precipitated white solid product was removed by filtration in the dark, and the fresh solutions of the aqua complexes were kept in a refrigerator and used in the further experiments.

2.4. Measurements

2.4.1. pH measurements

All pH measurements were realized at ambient temperature using an Iskra MA 5704 pH meter calibrated with Fischer certified buffer solutions of pH 4.00 and 7.00. The results were not corrected for the deuterium isotope effect.

2.4.2. NMR spectroscopy

The ^{1}H and ^{13}C NMR spectra were recorded on a Varian Gemini 2000 spectrometer (^{1}H at 200 MHz, ^{13}C at 50 MHz) using 5 mm NMR tubes. The NMR samples were prepared in D_2O as solvent and the total volume was 0.6 cm^3. Sodium trimethylsilylpropane-3-sulfonate (TSP) was used as an internal reference. The ^{1}H NMR spectra were acquired using the WATERGATE sequence for water suppression. Typical acquisition conditions were as follows: 90° pulses, 24 000 data number points, 4 s acquisition time, 1 s relaxation delay, collection of 16–128 transients and final digital resolution of 0.18 Hz per point. The ^{13}C NMR spectra were recorded with Waltz 16 ^{1}H broadband decoupling, 159 136 scans, 0.5 s relaxation delay, 1 s acquisition time, line broadening 1.0 Hz and 12 500 Hz spectral width. All the NMR spectra were processed using the Varian VNMR software (version 6.1, revision C). The chemical shifts are reported in ppm.

Fresh solutions of the aqua derivatives of dinuclear complexes **1**–**3** or their mononuclear $[Pt(X)(H_2O)_2]^{2+}$ analogues (X is 1,3-pd, 2,2-diMe-1,3-pd and 1,3-pnd, respectively) and Ac-L-Met-Gly and Ac-L-His-Gly dipeptides were prepared separately and then mixed in 1:1 molar ratio. The initial concentrations of dipeptide and aqua complex solutions were 40 mM. All reactions were performed in the pH range 2.0–2.5 at 37 °C. The rate constants were obtained from the ^{1}H NMR measurements. The values of the rate constants for the reactions between an equimolar amount of the given $[\{Pt(X)(H_2O)\}_2(\mu\text{-pz})]^{4+}$ complex and Ac-L-His-Gly dipeptide were determined when the data from the early part of the reaction (up to 2 h) were fitted to a second-order process [11] by plotting $x/a_o(a_o - x)$ against t (where a_o is the initial concentration of the Ac-L-His-Gly dipeptide and x is the concentration of the corresponding hydrolytically active Pt(II)-dipeptide $[\{Pt(X)(Ac\text{-L-His-Gly-}N3)\}(\mu\text{-pz})\{Pt(X)(H_2O)\}]^{4+}$ complex at time t). The concentration of the given Pt(II)-dipeptide complex was determined from the integral values of the resonances at 7.30 and 7.06 ppm, which correspond to the C5H imidazole protons of, respectively, free and monodentate coordinated through N3, the Ac-L-His-Gly dipeptide. Data was collected and analyzed using OriginPro 8 and Microsoft Office Excel 2007 programs.

2.4.3. UV–Vis spectrophotometry

The UV–Vis spectra for **1**–**3** were recorded on a Perkin Elmer Lambda 35 double-beam spectrophotometer equipped with thermostated 1.00 cm quartz Suprasil cells. The concentrations of the stock solutions of dinuclear Pt(II) complexes in water were 5×10^{-5} mol/dm^3. The spectra were recorded over the wavelength range 200–500 nm.

2.4.4. Elemental microanalyses

Elemental microanalyses for carbon, hydrogen and nitrogen parameters were performed by the Microanalytical Laboratory, Faculty of Chemistry, University of Belgrade.

2.5. X-ray analysis of *2* and *4*

Single crystals suitable for X-ray analysis were obtained only for **2** and **4**. Diffraction data for these complexes were measured with a Xcalibur kappa-geometry diffractometer using CrysAlisPro software [12] and monochromated Mo Kα radiation (λ = 0.71073 Å). Crystal data and experimental details are summarized in Table 1. The structures were solved by direct methods using SHELXS-86 [13] and refined by full-matrix least-squares calculations on F^2 with SHELXL-97 [13]. The intensity data were corrected for absorption effects [12]. Anisotropic displacement parameters were refined for all non-hydrogen atomic positions. Hydrogen atoms attached to the carbon and nitrogen atoms were placed in calculated positions (methyl C–H = 0.96, methylene C–H = 0.97, methine C–H = 0.98, aromatic C–H = 0.93 and amine N–H = 0.90 Å). Water hydrogens were located on difference Fourier maps and the O–H distances have been standardized to 0.85 Å. During the refinement, isotropic displacement parameters for H-atoms were assigned 20% higher than the isotropic equivalent for the atom to which the H-atom was bonded. All H-atoms were refined as riding. Owing to the disorder of the dinuclear $[\{Pt(1,3\text{-pnd})Cl\}_2(\mu\text{-pz})]^{2+}$ complex cation, which manifested in alternating positions of the ethyl substituent, the occupancy factors for the pairs of equivalent carbon atoms of these ethyl group were first refined freely with their sum constrained to unity, while the displacement parameters of the corresponding components of disorder were kept equivalent. The site occupation factor refined to 0.50(1) indicating 1:1 occupancy ratio. This value was kept fixed at the final stages of the refinement allowing the individual displacement parameters of the disorder components to vary. Multicomponent constitution of the investigated single crystals prompted us to evaluate whether these single crystals represent the whole bulk of the samples. For this purpose we have recorded the X-ray powder patterns for samples **2** and **4** and compared the obtained patterns with the corresponding patterns calculated on the basis of the known crystal structures, by utilizing a procedure included in the MERCURY [14] program. The measured and calculated powder patterns confirm the purity of the sample of **4**, but the experimental powder pattern of **2** contains an extra line at $2\theta = 9.276°$, suggestive of the presence of some impurity. The calculated and measured powder patterns are displayed in Fig. S1 of the Supporting information. SIEMENS [15] and MERCURY [14] computer graphics programs were used to prepare drawings.

Table 1
Crystal data for **2** and **4**.

	2	**4**
Crystal data		
Chemical formula	$(C_{14}H_{32}Cl_2N_6Pt_2)\cdot 2(H_8LiO_4)\cdot 4(Cl)\cdot 2(H_2O)$	$(C_{14}H_{32}Cl_2N_6Pt_2)\cdot 2(C_5H_{14}Cl_2N_2Pt)\cdot 2(Cl)\cdot 2(H_2O)$
M_r	1081.38	1588.81
Crystal system, space group	monoclinic, $P2_1/c$	triclinic, $P\bar{1}$
a, b, c (Å)	8.8468 (2), 13.2566 (2), 16.6892 (2)	7.5635 (3), 10.7877 (4), 14.0360(5)
α, β, γ (°)	90, 91.505 (1), 90	83.241 (3), 88.064 (3), 87.868 (3)
V (Å^3)	1956.61 (6)	1135.99 (7)
Z	2	1
μ (mm^{-1})	7.60	12.78
Crystal size (mm)	0.40 × 0.13 × 0.08	0.15 × 0.05 × 0.04
Data collection		
T_{min}, T_{max}	0.356, 1.000	0.645, 1.000
No. of measured, independent and observed $[I > 2\sigma(I)]$ reflections	41 298, 3457, 3090	18 859, 3996, 3011
R_{int}	0.033	0.058
$(\sin\theta/\lambda)_{max}$ (Å^{-1})	0.595	0.595
Refinement		
$R[F^2 > 2\sigma(F^2)]$, $wR(F^2)$, S	0.019, 0.041, 1.05	0.036, 0.065, 1.02
No. of reflections	3457	3996
No. of parameters	185	237
No. of restraints	0	37
$\Delta\rho_{max}$, $\Delta\rho_{min}$ (e Å^{-3})	0.85, −0.37	0.83, −0.64

3. Results and discussion

Four pyrazine (pz)-bridged Pt(II) complexes ([{Pt(1,3-pd)Cl}$_2$(μ-pz)]Cl$_2$·LiCl **(1)**, [{Pt(2,2-diMe-1,3-pd)Cl}$_2$(μ-pz)]Cl$_2$·2[Li(H$_2$O)$_4$]Cl·2H$_2$O (**2**), [{Pt(1,3-pnd)Cl}$_2$(μ-pz)](ClO$_4$)$_2$·H$_2$O (**3**) and [{Pt(1,3-pnd)Cl}$_2$(μ-pz)]Cl$_2$·2[Pt(1,3-pnd)Cl$_2$]·2H$_2$O (**4**); 1,3-pd = 1,3-propylenediamine, 2,2-diMe-1,3-pd = 2,2-dimethyl-1,3-propylenediamine and 1,3-pnd = (±)-1,3-pentanediamine) have been synthesized. Compounds **1**–**3** have been characterized by NMR (^{1}H and ^{13}C) spectroscopy, UV–Vis spectrophotometry and elemental microanalysis, while X-ray analysis has been applied for structure determination of **2** and **4,** for which suitable single crystals could be obtained. The catalytic activities of the aqua derivatives of **1**–**3**, with the general formulae [{Pt(X)(H$_2$O)}$_2$(μ-pz)]$^{4+}$, in the reactions with Ac-L-Met-Gly and Ac-L-His-Gly dipeptides have been investigated by applying ^{1}H NMR spectroscopy. The catalytic activities of the dinuclear aqua complexes **1**–**3** have been compared with those displayed by the corresponding mononuclear [Pt(X)(H$_2$O)$_2$]$^{2+}$ complexes (X is 1,3-pd, 2,2-diMe-1,3-pd and 1,3-pnd for **1**–**3**, respectively) with the same two dipeptides.

3.1. Complex characterization

3.1.1. X-ray crystallography

Single crystals suitable for X-ray analysis have been obtained only for **2** and **4**. The content of the multicomponent crystals of **2** and **4** is displayed in Figs. 1 and 2, respectively. Selected geometrical parameters for these complexes are compared in Table 2. Crystals of **2** consist of four different units, *i.e.* dinuclear [{Pt(2,2-diMe-1,3-pd)Cl}$_2$(μ-pz)]$^{2+}$ complex cation and lithium tetraaqua ion, chloride anions and water molecules as illustrated in Fig. 1. Crystals of **4** contain two types of Pt(II) complexes, mono- and dinuclear, of the formulae Pt(1,3-pnd)Cl$_2$ and [{Pt(1,3-pnd)Cl}$_2$(μ-pz)]$^{2+}$, respectively, chloride anions and water molecules. The constituents of this crystal lattice are displayed in (Fig. 2). In both crystal structures the pyrazine ligand displays a bidentate-bridging function leading to the formation of dinuclear complex cations of the general formulae [{Pt(X)Cl}$_2$(μ-pz)]$^{2+}$ (X is 2,2-diMe-1,3-pd and 1,3-pnd), and in both crystal structures these complexes are positioned on the inversion centers. Each of the two Pt(II) ions in the complex is surrounded by three nitrogen atoms and a chloride ion. Both mono- and dinuclear Pt(II) complexes display a square-planar geometry. In the cationic binuclear complexes the average values of the Pt–N bond lengths to the aliphatic and aromatic nitrogen atoms amount, respectively, to 2.037(5) and 2.027(3) Å.

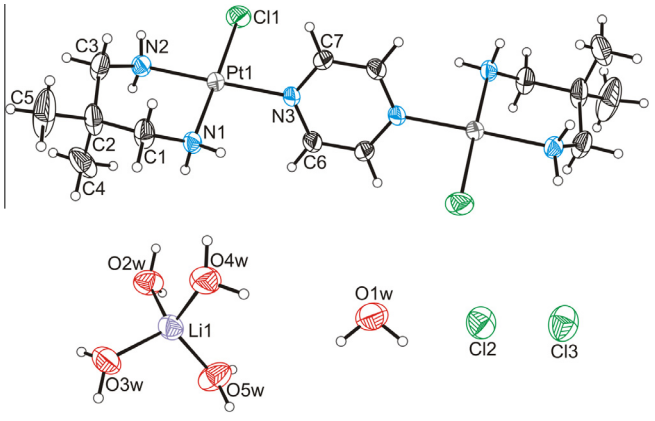

Fig. 1. Constituents of the multicomponent crystals of **2**. As the [{Pt(2,2-diMe-1,3-pd)Cl}$_2$(μ-pz)]$^{2+}$ cation occupies an inversion center, only the symmetry independent part of the complex is marked by labeled atoms. Displacement ellipsoids are drawn at 40% probability level and H-atoms are shown as spheres of arbitrary radii.

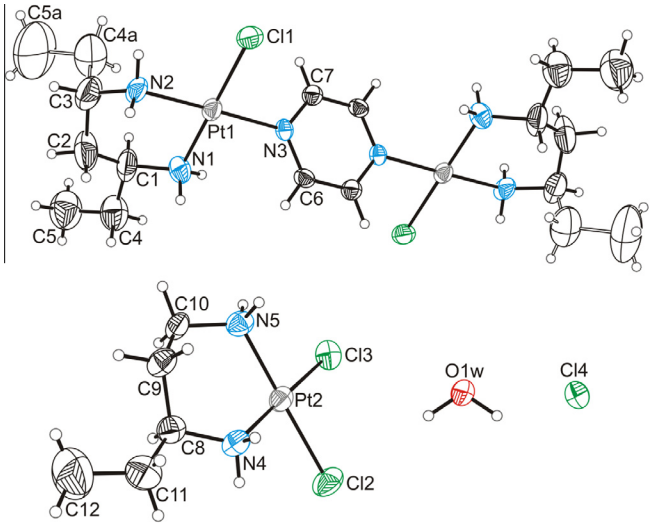

Fig. 2. Constituents of the multicomponent crystals of **4**. The crystal is a solid solution of stereoisomers of the [{Pt(1,3-pnd)Cl}$_2$(μ-pz)]$^{2+}$ complex cation (shown in Fig. 3) that occupy the same crystallographic site. This is manifested by alternating positions of the ethyl substituent distinguished here by bonds drawn with full and open lines. The full lines refer to the equatorial and the open lines to the axial orientation of the ethyl substituent. As the [{Pt(1,3-pnd)Cl}$_2$(μ-pz)]$^{2+}$ cation occupies an inversion center, only the symmetry independent part of the complex is marked by labeled atoms. Displacement ellipsoids are drawn at 40% probability level and H-atoms are shown as spheres of arbitrary radii.

The chelate rings adopt a chair conformation, significantly flattened at the coordination site. The N–Pt–N angles in the six-membered chelate rings (91.8(3) and 90.8(1)°) present a major difference from those forming the five-membered rings in which this angle reduces to 82.8(2)° [2].

In the multicomponent crystal of **4** the site occupied by the [{Pt(1,3-pnd)Cl}$_2$(μ-pz)]$^{2+}$ cation is disordered. The disorder can be modelled in two different ways that, in principle, might mirror the presence at one site of four distinct stereoisomers illustrated in Fig. 3. The stereoisomerism arises from the presence of stereogenic center at one of the carbon atoms forming 1,3-propylenediamine ring and from distinction to which of the two ring nitrogens this carbon atom is attached. We differentiate the two nitrogen atoms by their positioning with respect to the coordinated chloride, as either *trans* (N1) or *cis* (N2). In the six-membered 1,3-propylenediamine ring ethyl substituent attached to the carbon atom proximal to N1 adopts an equatorial position, while the one attached to the carbon atom proximal to N2 is axial. With regards to the configuration at the two carbon stereogenic centers, all stereoisomers that mirror the electron density distribution at this site possess the *R*,*S* or *S*,*R* configuration. Of four stereoisomers that fit to the atomic positions obtained from the X-ray analysis, two display C_i symmetry, *i.e.* they are either *trans*,*trans*-(*R*,*S*) or *cis*,*cis*-(*R*,*S*) (Fig. 3a and b). Another two belong to asymmetrical *trans*-(*S*), *cis*-(*R*) and *cis*-(*S*), *trans*-(*R*), isomers (Fig. 3c and d), randomly distributed around the inversion center at this site in crystal. Contribution of each type of the four possible stereoisomers to the superposition picture that comes out from the electron density map could not be established on the grounds of X-ray analysis. However, by solving this crystal structure we were able to demonstrate that preparation of the monodimethylformamide (dmf) complex [Pt(1,3-pnd)Cl(dmf)]NO$_3$ and consequent formation of the dimetallic pyrazine complex did not proceed regiospecifically, as either of the two chloride ligands was predisposed to play a role of a leaving group. As a consequence, we have obtained a mixture of stereoisomeric products which showed the unexpected property of preferentially crystallizing together in a form of substitutional solid solution.

Table 2
Selected geometrical parameters (Å, °).

[{Pt(2,2-diMe-1,3-pd)Cl}$_2$(μ-pz)]$^{2+}$		[{Pt(1,3-pnd)Cl}$_2$(μ-pz)]$^{2+}$	
Pt1···Pt1^i	6.8250 (2)	Pt1···Pt1^i	6.8137 (6)
Angle between coordination plane and the pz plane	58.5 (2)	Angle between coordination plane and the pz plane	56.4 (2)
N1–Pt1	2.041 (2)	N1–Pt1	2.041 (6)
N2–Pt1	2.030 (2)	N2–Pt1	2.035 (6)
N3–Pt1	2.030 (2)	N3–Pt1	2.024 (6)
Cl1–Pt1	2.2991 (9)	Cl1–Pt1	2.298 (2)
N3–Pt1–N2	178.27 (10)	N3–Pt1–N2	176.9 (3)
N3–Pt1–N1	90.81 (10)	N3–Pt1–N1	89.0 (2)
N2–Pt1–N1	90.84 (10)	N2–Pt1–N1	91.8 (3)
N3–Pt1–Cl1	90.21 (8)	N3–Pt1–Cl1	91.04 (17)
N2–Pt1–Cl1	88.15 (8)	N2–Pt1–Cl1	88.1 (2)
N1–Pt1–Cl1	178.77 (8)	N1–Pt1–Cl1	179.9 (2)
N1–C1–C2–C3	−67.0(5)	N1–C1–C2–C3	65.7(13)
C1–C2–C3–N2	65.4(5)	C1–C2–C3–N2	−69.4(13)
C2–C3–N2–Pt1	−58.9 (4)	C2–C3–N2–Pt1	56.7 (10)
C3–N2–Pt1–N1	42.2 (3)	C3–N2–Pt1–N1	−38.4 (7)
N2–Pt1–N1–C1	−42.9 (2)	N2–Pt1–N1–C1	33.9 (7)
Pt1–N1–C1–C2	60.8 (4)	Pt1–N1–C1–C2	−50.0 (11)
[Pt(1,3-pnd)Cl$_2$]			
N4–Pt2	2.039 (7)	Cl2–Pt2	2.306 (2)
N5–Pt2	2.044 (6)	Cl3–Pt2	2.308 (2)
N4–Pt2–N5	92.4 (3)	N4–Pt2–Cl3	178.3 (2)
N4–Pt2–Cl2	86.51 (19)	N5–Pt2–Cl3	88.1 (2)
N5–Pt2–Cl2	177.9 (2)	Cl2–Pt2–Cl3	92.88 (9)
N4–C8–C9–C10	71.6(9)	C10–N5–Pt2–N4	−35.6(6)
C8–C9–C10–N5	−71.7(10)	N5–Pt2–N4–C8	38.2(6)
C9–C10–N5–Pt2	55.6(9)	Pt2–N4–C8–C9	−58.1(9)

Symmetry code(s): (i) $-x+1, -y, -z+1$.

In both investigated crystal structures there are numerous N–H···Cl, N–H···O and O–H···Cl hydrogen bonds, which together with electrostatic interactions take part in the cohesion of the investigated crystals. Two types of hydrogen-bonding interactions can be distinguished, namely direct N–H···Cl hydrogen bonds between metal complexes or between ligand amine and Cl^- ion, and water-bridged hydrogen bonding from amine group to a water molecule and then to the Cl^- ion. Hydrogen bond parameters are listed in Table S1 of SI.

3.1.2. NMR spectroscopy

The ^{1}H and ^{13}C NMR chemical shifts of free diamine (1,3-pd, 1,3-pnd and 2,2-diMe-1,3-pd) and pyrazine ligands and those for these ligands coordinated to Pt(II) in the corresponding [{Pt(X)Cl}$_2$(μ-pz)]$^{2+}$ complexes **1**–**3** are listed in Table 3. The NMR chemical shifts for complexes **1** and **2** have been previously reported [9] and here these spectral data have been repeated and discussed in comparison with those for the uncoordinated diamine ligands and complex **3**. All chemical shifts for the uncoordinated diamine X and pz ligands generally agree with the literature values [16]. After chelation of 1,3-pd ligand to Pt(II) in complex **1** its two ^{1}H NMR multiplets centered at 1.60 and 2.65 ppm for middle C2 and terminal C1 and C3 methylene protons, respectively, are shifted downfield ($\Delta\delta$ = 0.29 for C2 and 0.14 ppm for C1 and C3 methylene protons). Downfield shifting of two signals for middle and terminal carbon atoms of 1,3-pd was also observed in the ^{13}C NMR spectrum of the corresponding Pt(II) complex. Moreover, a signal for C1 and C3 terminal carbon atoms of 1,3-pd at 39.40 ppm was split into two (44.55 and 45.66 ppm), which demonstrates that upon coordination to Pt(II) the two carbon nuclei are found in different chemical environments, similarly as the nitrogen nuclei to which they are attached, *i.e.* upon coordination, one of these nitrogen atoms becomes *cis* and the other *trans* oriented with respect to the coordinated chloride. Not surprisingly the downfield shifting upon coordination to the Pt(II) center was also observed for **2** (Table 3) and the ^{1}H NMR spectrum of 2,2-diMe-1,3-pd ligand became more complex. The singlet at 0.84 ppm for two CH_3 groups was shifted downfield to 1.01 ppm while that at 2.41 ppm for C1 and C3 terminal methylene protons of free 2,2-diMe-1,3-pd ligand was split into two singlets (2.38 and 2.49 ppm). Also observed was the splitting of the carbon-13 resonance at 51.69 ppm for C1 and C3 terminal carbon atoms, again displaying stereochemical and environmental non-equivalence of the two carbons (Table 3).

All ^{1}H NMR resonances for complex **3** were shifted downfield in respect to those for the uncoordinated 1,3-pnd ligand. The triplet at 0.86 ppm for C5 methyl protons of the free ligand, after coordination to Pt(II) ion was split into two triplets at 0.93 and 1.00 ppm, which overlap into doublet of triplets. Two remaining multiplets in this spectrum at larger chemical shifts were assigned to C2 and C4 methylene protons (1.82 ppm), and to C1 methylene and C3 methine protons (2.82 ppm). In the ^{13}C NMR spectrum of the free 1,3-pnd ligand five peaks were observed in the region of 12–53 ppm indicating the nonequivalence of all carbons. The peaks at 12.08 and 31.94 ppm were assigned to the C5 methyl and C4 methylene carbon resonances of ethyl group, respectively. The peak at 40.27 ppm was assigned to the middle C2 methylene carbon atom, while the remaining two peaks at 41.49 and 52.02 ppm were assigned to the terminal C1 methylene and C3 methine carbon resonances of 1,3-propylenediamine chain, respectively. After coordination of 1,3-pnd to the Pt(II) ion in complex **3** its ^{13}C NMR spectrum becomes more complex. Thus, two resonances for C5 methyl and C2 methylene carbon atoms were split into two pairs of signals at 11.93 and 12.04 ppm for C5 and 42.84 and 42.94 ppm for C2 atoms. However, each of the resonances for C1, C3 and C4 carbons in complex **3** was split into four signals, almost all shifted downfield in respect to those for the free 1,3-pnd ligand. The appearance of four distinct resonances for C1, C3 and C4 carbon atoms can be explained by assuming the

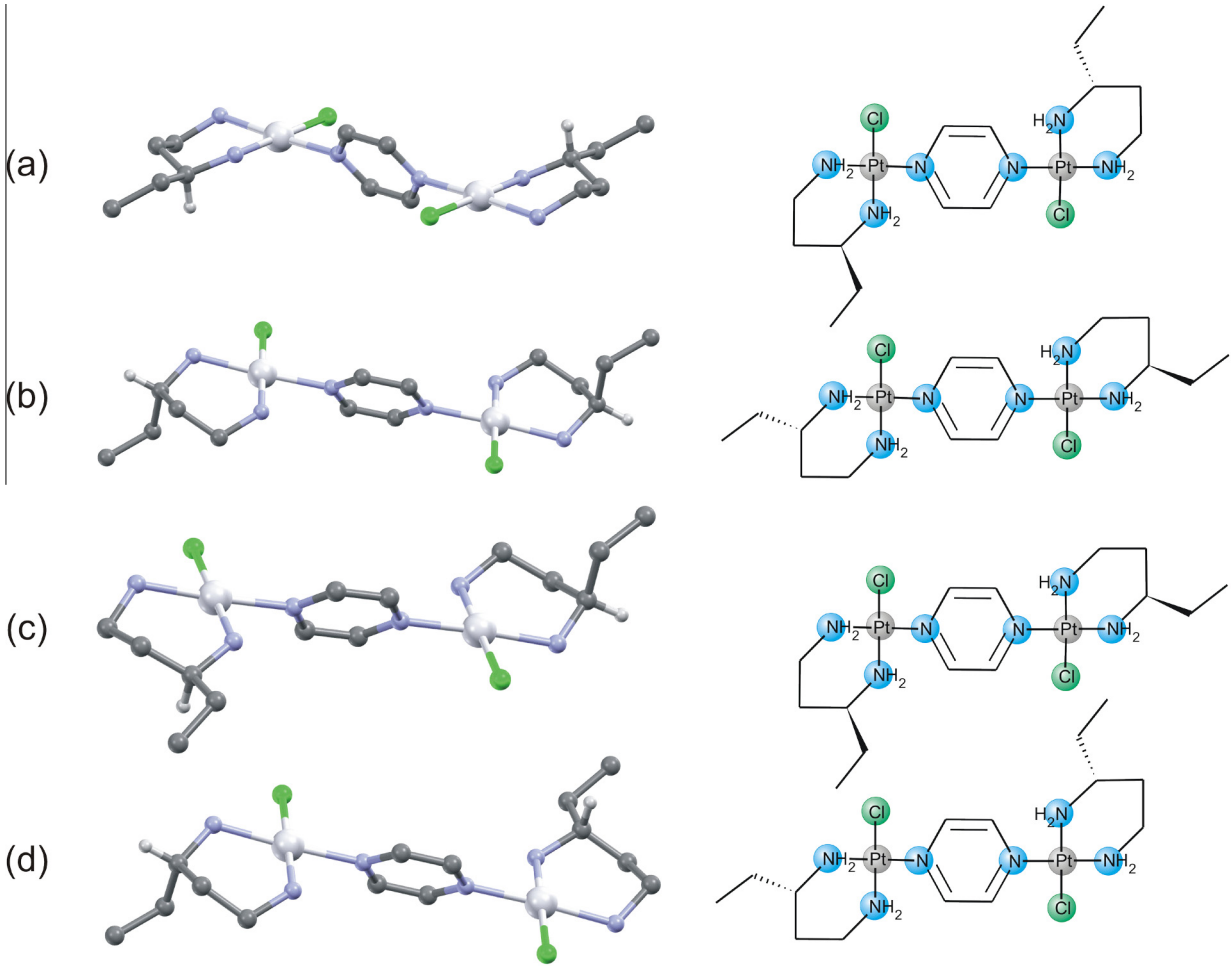

Fig. 3. *trans,cis*-(*S,R*) Stereoisomers of the $[\{Pt(1,3\text{-pnd})Cl\}_2(\mu\text{-pz})]^{2+}$ complex cation, whose possible presence in the crystal lattice is consistent with the observed electron density distribution: *trans,trans*-(*S,R*) (a), *cis,cis*-(*S,R*) (b), *trans,cis*-(*S,R*) (c) and *cis,trans*-(*S,R*) (d).

Table 3
^{1}H and ^{13}C NMR chemical shifts (δ, ppm) for the free 1,3-pd, 2,2-diMe-1,3-pd and 1,3-pnd ligands and the corresponding pyrazine-bridged Pt(II) complexes **1**–**3**, respectively, in D_2O as solvent with TSP as the internal standard.

Diamine (X)/Pt(II) complex[a]	^{1}H NMR	^{13}C NMR
	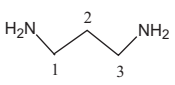 1,3-pd	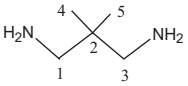 2,2-diMe-1,3-pd
		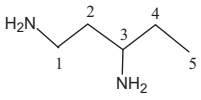 1,3-pnd
1,3-pd	1.60 (*m*, C2), 2.65 (*m*, C1 and C3)	28.52 (C2), 39.40 (C1 and C3)
$[\{Pt(1,3\text{-pd})Cl\}_2(\mu\text{-pz})]^{2+}$[b] (**1**)	1.89 (*m*, C2), 2.79 (*m*, C1 and C3), 9.02 (*s*, pz)	29.82 (C2), 44.55, 45.66 (C1 and C3) 153.56 (pz)
2,2-diMe-1,3-pd	0.84 (*s*, C4 and C5), 2.41 (*s*, C1 and C3)	24.72 (C4 and C5), 35.81 (C2), 51.69 (C1 and C3)
$[\{Pt(2,2\text{-diMe-}1,3\text{-pd})Cl\}_2(\mu\text{-pz})]^{2+}$[b] (**2**)	1.01 (*s*, C4 and C5), 2.38 and 2.49 (2*s*, C1 and C3), 9.05 (*s*, pz)	25.57 (C4 and C5), 36.14 (C2), 53.97, 54.99 (C1 and C3), 153.58 (pz)
1,3-pnd	0.86 (*t*, C5), 1.45 (*m*, C2 and C4), 2.66 (*m*, C1 and C3)	12.08 (C5), 31.94 (C4), 40.27 (C2), 41.49 (C1), 52.02 (C3)
$[\{Pt(1,3\text{-pnd})Cl\}_2(\mu\text{-pz})]^{2+}$ (**3**)	0.93, 1.00 (*dt*, C5), 1.82 (*m*, C2 and C4), 2.82 (*m*, C1 and C3), 9.06 (*s*, pz)	11.93,12.04 (C5), 30.12, 30.28,33.21, 33.54 (C4), 42.84, 42.94 (C2), 43.26, 43.36, 43.73, 43.78 (C1), 56.18, 56.25, 57.14, 57.27 (C3), 153.62 (pz)

[a] ^{1}H and ^{13}C NMR chemical shifts of free pz are at 8.66 (*s*) and 143.86 ppm, respectively.
[b] Ref [9].

presence of four distinct stereoisomeric products of **3**. The existence of such mixture of stereoisomers in a crystal has been indicated by the X-ray analysis of complex **4**, see Fig. 3.

In the aromatic region of the ^{1}H NMR spectra of investigated dinuclear Pt(II) complexes a singlet corresponding to the bridging pyrazine ligand was detected in the range 9.02–9.06 ppm (Table 3). This is in accordance with data previously reported for similar dinuclear Pt(II) complexes [1,8,16]. Four protons of uncoordinated pyrazine appear as a singlet at 8.66 ppm and this singlet is being shifted downfield after bidentate coordination of pyrazine to two

equivalent mononuclear Pt(II) units. Free pyrazine shows carbon-13 signal at 143.86 ppm, which after bidentate coordination to Pt(II) shifts downfield to 153.56–153.71 ppm.

3.1.3. UV–Vis spectrophotometry

A typical plot of the UV–Vis spectra of **1**–**3** is given in Fig. 4. All complexes have absorption maxima within a wavelength range of 280–290 and shoulders in the range of 340–360 nm. These spectra have been compared with those for the analogous $[\{Pt(en)Cl\}_2(\mu\text{-pz})]Cl_2$ complex. The crystal structure of this complex has been previously reported [1] and herein its UV–Vis spectrum is presented as a reference. As it can be seen in Fig. 4, the spectra of all presently investigated Pt(II) complexes are almost identical with that of $[\{Pt(en)Cl\}_2(\mu\text{-pz})]Cl_2$ of the known crystal structure indicating that they have bidentate coordinated diamine ligand and pyrazine ligand bridging two equivalent Pt(II) units.

3.2. Hydrolytic reactions of pyrazine-bridged Pt(II) complexes with Ac-L-Met-Gly and Ac-L-His-Gly dipeptides

The pyrazine (pz)-bridged Pt(II) complexes **1**–**3** were converted into the corresponding aqua species, $[\{Pt(X)(H_2O)\}_2(\mu\text{-pz})]^{4+}$ (X is 1,3-pd, 2,2-diMe-1,3-pd and 1,3-pnd, respectively), and their catalytic activities in the hydrolytic cleavage of Ac-L-Met-Gly and Ac-L-His-Gly dipeptides were investigated by ^{1}H NMR spectroscopy. The rate of hydrolysis of these two dipeptides in the presence of $[\{Pt(X)(H_2O)\}_2(\mu\text{-pz})]^{4+}$ complexes with six-membered diamine ring (X) were compared with those for $[\{Pt(en)(H_2O)\}_2(\mu\text{-pz})]^{4+}$ complex having five-membered diamine ring [1,2]. All these reactions were carried out with an equimolar amounts of the Pt(II) complex and corresponding dipeptide in the pH range 2.0–2.5 at 37 °C. As it was shown in our previous studies [17–20], acidic solutions are needed to suppress the formation of hydroxo-bridged oligomeric Pt(II) complexes, which are catalytically inactive. All $[\{Pt(X)(H_2O)\}_2(\mu\text{-pz})]^{4+}$ complexes were stable under the above mentioned experimental conditions. Thus, no elimination of the bridging-pyrazine ligand or opening of diamine ring X was observed during 24 h of the reaction time. However, when the reactions of $[\{Pt(X)(H_2O)\}_2(\mu\text{-pz})]^{4+}$ with Ac-L-Met-Gly and Ac-L-His-Gly dipeptides were followed for more than 24 h, some changes in the aromatic region of the ^{1}H NMR spectrum were observed. The singlet appeared in the region at 9.02–9.06 ppm for the bridging pyrazine ligand of $[\{Pt(X)(H_2O)\}_2(\mu\text{-pz})]^{4+}$ complex (chemical shifts of this singlet is dependent from the type of Pt(II) complex) decreased while two symmetric multiplets in the range 8.75–9.00 ppm increased. The appearance of these two new multiplets indicates that one Pt(II)–N(pyrazine) bond of Pt(II) complex was broken and that the four pyrazine protons of this ligand coordinated in a monotopic fashion to Pt(II) ion were split into two multiplets because of vicinal and long-range coupling [1,8,16].

3.2.1. Ac-L-Met-Gly

When an equimolar amount of $[\{Pt(X)(H_2O)\}_2(\mu\text{-pz})]^{4+}$ was incubated with Ac-L-Met-Gly, under the above mentioned experimental conditions, all reactions ended up with the formation of the platinum(II)-dipeptide $[\{Pt(X)(Ac\text{-L-Met-Gly-}S)\}(\mu\text{-pz})\{Pt(X)(H_2O)\}]^{4+}$ complex (Fig. 5a) in a yield of more than 95% achieved in less than 30 min. Formation of this intermediate product was detected by the simultaneous decline of the proton NMR resonance at 2.11 ppm, arising from the *S*-methyl protons of free Ac-L-Met-Gly, and the growth of the resonance at 2.45–2.55 ppm, corresponding to the protons of the dipeptide coordinated to Pt(II) through the sulfur atom. These chemical shifts are in accordance with those previously reported for the reactions of Pt(II) complexes with different methionine-containing molecules [20–22]. In all investigated reactions the $[\{Pt(X)(Ac\text{-L-Met-Gly-}S)\}(\mu\text{-pz})\{Pt(X)(H_2O)\}]^{4+}$ complex is hydrolytically active and promotes the selective cleavage of the Met-Gly amide bond in the Ac-L-Met-Gly dipeptide. The ^{1}H NMR resonance at 4.02 ppm corresponding to the glycine protons of the Ac-L-Met-Gly dipeptide attached to the Pt(II) decreased, while that at 3.76 ppm for the free glycine increased (Fig. S2 of SI). Upon addition of glycine to the reaction mixture the resonance at 3.76 ppm was enhanced confirming the presence of uncoordinated glycine molecules. The amount of the hydrolytic product was determined from the known initial concentration of Ac-L-Met-Gly (which was almost equal to the concentration of $[\{Pt(X)(Ac\text{-L-Met-Gly-S})\}(\mu\text{-pz})\{Pt(X)(H_2O)\}]^{4+}$ complex) and from the integrated resonance for the methylene protons of the free glycine. We have found that during the first 6 h the pyrazine-bridged Pt(II) complex with the five-membered ethylenediamine ring was better promoter of the hydrolytic cleavage of the Met-Gly amide bond than any of the presently investigated $[\{Pt(X)(H_2O)\}_2(\mu\text{-pz})]^{4+}$ complexes, all having the six-membered diamine ring X. No significant difference in the catalytic activities between 1,3-pd, 1,3-pnd and 2,2-diMe-1,3-pd dinuclear Pt(II)

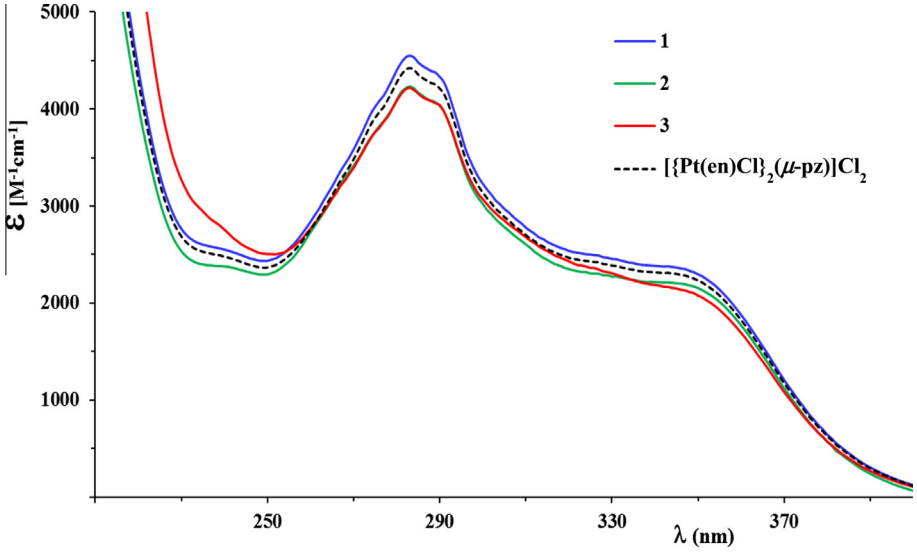

Fig. 4. UV–Vis spectra of investigated complexes **1**–**3**. These spectra were compared with that for $[\{Pt(en)Cl\}_2(\mu\text{-pz})]Cl_2$ complex of the known crystal structure [1].

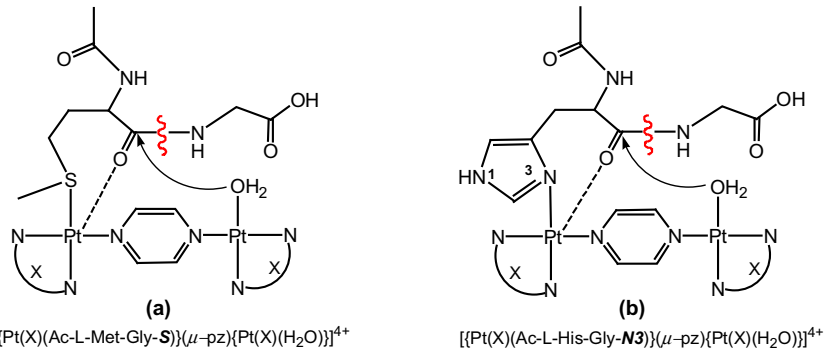

Fig. 5. Schematic presentation of the hydrolytically active platinum(II)-peptide complexes observed in the reaction of aqua derivatives of **1**–**3** with Ac-L-Met-Gly (a) and Ac-L-His-Gly (b) at pH 2.0–2.5 and 37 °C.

complexes was observed during the 6 h time. However, when these reactions were prolonged for up to 24 h the amount of hydrolyzed Met-Gly amide bond achieved 85–90% for all Pt(II) complexes, indicating that hydrolysis of the dipeptide has been almost completed (Fig. 6a). Our recently published results obtained for a series of dinuclear $[\{Pt(X)(H_2O)\}_2(\mu\text{-pz})]^{4+}$ complexes (X is ethylenediamine, en; (±)-1,2-propylenediamine, 1,2-pn; isobutylenediamine, ibn; and *trans*-(±)-1,2-diaminocyclohexane, dach) pointed to a steady decrease of the amount of the hydrolyzed Ac-L-Met-Gly dipeptide with an increase of the steric hindrance within the five-membered chelate ring (X) (en > 1,2-pn > ibn > -dach) [3]. Conversely, our present results indicate that steric modification of the six-membered diamine ring in $[\{Pt(X)(H_2O)\}_2(\mu\text{-pz})]^{4+}$ complexes (X is 1,3-pd, 2,2-diMe-1,3-pd and 1,3-pnd) has no significant influence on the rate of the hydrolysis of Ac-L-Met-Gly dipeptide, see Fig. 6a.

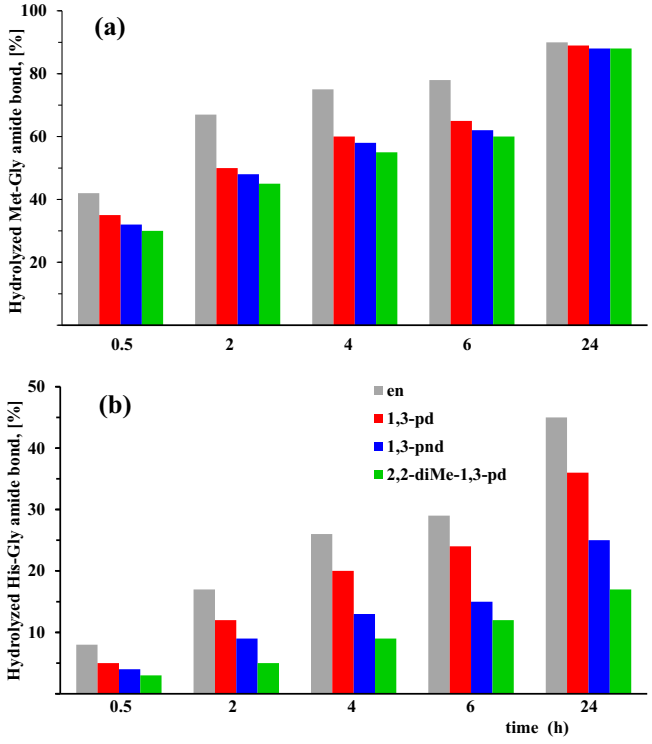

Fig. 6. Time dependence of the hydrolytic cleavage of Ac-L-Met-Gly (a) and Ac-L-His-Gly (b) in the presence of an equimolar amount of aqua derivatives of **1**–**3** at pH 2.0–2.5 and 37 °C. The catalytic activities of investigated complexes are compared with that for $[\{Pt(en)(H_2O)\}_2(\mu\text{-pz})]^{4+}$ complex reported in literature [1,2].

3.2.2. Ac-L-His-Gly

When an equimolar amount of $[\{Pt(X)(H_2O)\}_2(\mu\text{-pz})]^{4+}$ was incubated with Ac-L-His-Gly dipeptide for 24 h and in the pH range 2.0–2.5 at 37 °C, only one NMR detectable $[\{Pt(X)(Ac\text{-L-His-Gly-}N3)\}(\mu\text{-pz})\{Pt(X)(H_2O)\}]^{4+}$ complex was observed in the reaction mixture (see Fig. 5b). As it is shown in this figure, the $[\{Pt(X)(Ac\text{-L-His-Gly-}N3)\}(\mu\text{-pz})\{Pt(X)(H_2O)\}]^{4+}$ complex contains the Ac-L-His-Gly dipeptide monodentate coordinated *via* the imidazole N3 atom. No coordination to N1 imidazole nitrogen was observed. The formation of this Pt(II)-dipeptide complex was evidenced by the appearance of new resonances in the ^{1}H NMR spectrum at 8.08 and 7.06 ppm corresponding to the C2H and C5H imidazole protons, respectively, and by the simultaneous decrease of the resonances at 8.58 and 7.30 ppm, which correspond to the resonances of these two protons in a free dipeptide. The chemical shifts of the C2H and C5H imidazole protons of the $[\{Pt(X)(Ac\text{-L-His-Gly-}N3)\}(\mu\text{-pz})\{Pt(X)(H_2O)\}]^{4+}$ are in accordance to those for the reaction of Ac-L-His-Gly dipeptide with mononuclear $[Pt(en)(H_2O)_2]^{2+}$ [17,20,23,24] and dinuclear $[\{Pt(en)(H_2O)\}_2(\mu\text{-pz})]^{4+}$ [2] complexes, all displaying a monodentate coordination of the dipeptide through the N3 imidazole nitrogen atom. The given $[\{Pt(X)(Ac\text{-L-His-Gly-}N3)\}(\mu\text{-pz})\{Pt(X)(H_2O)\}]^{4+}$ complex is an intermediate product which promotes cleavage of the His-Gly amide bond in Ac-L-His-Gly dipeptide attached to the Pt(II). This hydrolytic reaction can be successfully followed by observing changes in the ^{1}H NMR spectrum in time (Fig. S2 of SI). As the time passes, the resonance at 3.92 ppm, which belongs to the methylene glycine protons of the uncoordinated Ac-L-His-Gly as well as to the same protons in the $[\{Pt(X)(Ac\text{-L-His-Gly-}N3)\}(\mu\text{-pz})\{Pt(X)(H_2O)\}]^{4+}$ type of complex, decreases while a new resonance at 3.62 ppm from the free glycine increases. Upon addition of glycine to the reaction mixture, the resonance at 3.62 ppm has been markedly enhanced. The concentration of free glycine resulting from this hydrolytic process was determined from the known initial concentration of Ac-L-His-Gly dipeptide (this concentration is equal to the sum of concentrations of $[\{Pt(X)(Ac\text{-L-His-Gly-}N3)\}(\mu\text{-pz})\{Pt(X)(H_2O)\}]^{4+}$ complex and uncoordinated Ac-L-His-Gly) and from the integrated resonance of the free glycine. We have compared the catalytic activities in the cleavage of the Ac-L-His-Gly dipeptide for $[\{Pt(X)(H_2O)\}_2(\mu\text{-pz})]^{4+}$ type complexes with those displayed by the previously investigated $[\{Pt(en)(H_2O)\}_2(\mu\text{-pz})]^{4+}$ complex [2] (Table 4). The time dependence of the hydrolytic cleavage of the His-Gly peptide bond in reactions between different dinuclear $[\{Pt(X)(H_2O)\}_2(\mu\text{-pz})]^{4+}$ complexes and Ac-L-His-Gly dipeptide is given in Fig. 6b. From this figure it can be concluded that the amount of the hydrolyzed Ac-L-His-Gly dipeptide decreased in the following order: en > 1,3-pd > 1,3-pnd > 2,2-diMe-1,3-pd. This difference in the hydrolytic ability of the investigated dinuclear $[\{Pt(X)(H_2O)\}_2(\mu\text{-pz})]^{4+}$ type complexes can be correlated with their

Table 4
Second-order rate constants for formation of the hydrolytically active platinum(II)-peptide $[\{Pt(X)(Ac\text{-}L\text{-}His\text{-}Gly\text{-}N3)\}(\mu\text{-}pz)\{Pt(X)(H_2O)\}]^{4+}$ complex in the reactions of $[\{Pt(X)(H_2O)\}_2(\mu\text{-}pz)]^{4+}$ complexes (X is en, 1,3-pd, 2,2-diMe-1,3-pd and 1,3-pnd) with Ac-L-His-Gly dipeptide. The rate constants were correlated with the amount of hydrolyzed His-Gly amide bond observed after 24 h, [%]. All reactions were performed in the pH range 2.0–2.5 at 37 °C.

Complex	k_2, $10^3 k_2/M^{-1}\,s^{-1}$	Hydrolyzed His-Gly, [%]
$[\{Pt(en)(H_2O)\}_2(\mu\text{-}pz)]^{4+}$	2.08 ± 0.06	45
$[\{Pt(1,3\text{-}pd)(H_2O)\}_2(\mu\text{-}pz)]^{4+}$	1.58 ± 0.05	36
$[\{Pt(1,3\text{-}pnd)(H_2O)\}_2(\mu\text{-}pz)]^{4+}$	1.09 ± 0.09	25
$[\{Pt(2,2\text{-}diMe\text{-}1,3\text{-}pd)(H_2O)\}_2(\mu\text{-}pz)]^{4+}$	0.87 ± 0.01	17

reactivity with Ac-L-His-Gly. Second-order rate constants for the reactions leading to the formation of the hydrolytically active $[\{Pt(X)(Ac\text{-}L\text{-}His\text{-}Gly\text{-}N3)\}(\mu\text{-}pz)\{Pt(X)(H_2O)\}]^{4+}$ complex are presented in Table 4. It can be seen from this table that the values of the rate constants for these reactions decreased in the same order as the amount of the hydrolyzed His-Gly amide bond. This is in accord with the observation that reactivity of Ac-L-His-Gly with $[\{Pt(X)(H_2O)\}_2(\mu\text{-}pz)]^{4+}$ complexes can be correlated with structural modification of the diamine X ligand. This type of ligand contributes to the steric bulk of the dinuclear Pt(II) complex hindering the approach of the N3 imidazole atom of the histidine residue to the metal center and consequent formation of hydrolytically active $[\{Pt(X)(Ac\text{-}L\text{-}His\text{-}Gly\text{-}N3)\}(\mu\text{-}pz)\{Pt(X)(H_2O)\}]^{4+}$ complex. Kinetic data presented in Table 4 confirmed that presently investigated hydrolytic reaction can be inhibited by increasing the size of the X ring from five- in ethylenediamine to six-membered in 1,3-propylenediamine and/or by incorporation of ethyl (1,3-pnd) or two methyl groups (2,2-diMe-1,3-pd) to the 1,3-propylenediamine chain.

Furthermore, we compared hydrolytic activity between dinuclear aqua derivatives of **1**–**3** and the corresponding mononuclear $[Pt(X)(H_2O)_2]^{2+}$ complexes (X is 1,3-pd, 2,2-diMe-1,3-pd and 1,3-pnd, respectively), in their reactions with Ac-L-Met-Gly and Ac-L-His-Gly dipeptides. All reactions were performed under the above mentioned experimental conditions. Differences in the amount of the hydrolyzed amide bond [%] in these dipeptides are given in Table 5. From this table it can be seen that each dinuclear Pt(II)-aqua complex in comparison with the analogue mononuclear complex showed better catalytic activity in the hydrolysis of Met-Gly and His-Gly amide bonds of Ac-L-Met-Gly and Ac-L-His-Gly dipeptides, respectively. These results are in accordance with those reported recently for the reaction of dinuclear $[\{Pt(en)(H_2O)\}_2(\mu\text{-}pz)]^{4+}$ and mononuclear $[Pt(en)(H_2O)_2]^{2+}$ complexes with Ac-L-Met-Gly dipeptide [1]. The better catalytic activity of dinuclear $[\{Pt(X)(H_2O)\}_2(\mu\text{-}pz)]^{4+}$ complexes in comparison to their analogue mononuclear units can be explained by the facts that two Pt(II) centers in these dinuclear complexes could simultaneously participate in the cleavage of the scissile amide bond, one by polarizing the carbonyl oxygen atom and another by delivering a water molecule (see Fig. 5a and b). However, the single Pt(II) ion in the mononuclear $[Pt(X)(H_2O)_2]^{2+}$ complexes is incapable in promoting these two interactions simultaneously.

Table 5
Comparison of the hydrolytic activity between dinuclear $[\{Pt(X)(H_2O)\}_2(\mu\text{-}pz)]^{4+}$ and the corresponding mononuclear $[Pt(X)(H_2O)_2]^{2+}$ complexes (X is 1,3-pd, 2,2-diMe-1,3-pd and 1,3-pnd) in the reaction with Ac-L-Met-Gly and Ac-L-His-Gly dipeptides. All reactions were performed at the pH 2.0–2.5 and at 37 °C.

Mononuclear/dinuclear Pt(II) complex	The amount [%] of the hydrolyzed dipeptide Ac-L-Met-Gly (24 h)	Ac-L-His-Gly (72 h)
$[Pt(1,3\text{-}pd)(H_2O)_2]^{2+}$	55	35
$[\{Pt(1,3\text{-}pd)(H_2O)\}_2(\mu\text{-}pz)]^{4+}$	89	60
$[Pt(2,2\text{-}diMe\text{-}1,3\text{-}pd)(H_2O)_2]^{2+}$	54	31
$[\{Pt(2,2\text{-}diMe\text{-}1,3\text{-}pd)(H_2O)\}_2(\mu\text{-}pz)]^{4+}$	88	50
$[Pt(1,3\text{-}pnd)(H_2O)_2]^{2+}$	54	31
$[\{Pt(1,3\text{-}pnd)(H_2O)\}_2(\mu\text{-}pz)]^{4+}$	88	55

4. Conclusions

Our investigations of the reactions of pyrazine (pz)-bridged $[\{Pt(X)(H_2O)\}_2(\mu\text{-}pz)]^{4+}$ complexes (X is chelated diamine ligand 1,3-propylenediamine, 1,3-pd; (±)-1,3-pentanediamine, 1,3-pnd; and 2,2-dimethyl-1,3-propylenediamine, 2,2-diMe-1,3-pd) with Ac-L-Met-Gly and Ac-L-His-Gly showed that all these complexes promote selective cleavage of the amide bond involving carboxylic group of the anchoring amino acid methionine and histidine in the investigated N-acetylated dipeptides. Furthermore, it was demonstrated that the investigated complexes are more reactive with methionine- than histidine-containing dipeptides and that structural modification of the diamine ligand X has no measurable effect on the catalytic activity of the $[\{Pt(X)(H_2O)\}_2(\mu\text{-}pz)]^{4+}$ complexes in the 24 h lasting process of hydrolysis of the Met-Gly amide bond of Ac-L-Met-Gly dipeptide. This contrasts with the observed differentiation of the catalytic activity of these complexes in the process of hydrolysis of Ac-L-His-Gly dipeptide. More specifically, the amount of the hydrolyzed Ac-L-His-Gly dipeptide decreased with an increasing steric hindrance in the chelated diamine ligand X in the following order en > 1,3-pd > 1,3-pnd > 2,2-diMe-1,3-pd. All investigated dinuclear Pt(II)-aqua complexes are better catalytic agents in the hydrolysis of the dipeptides than the analogous mononuclear Pt(II)-aqua complexes.

Acknowledgements

This work was funded in part by the Ministry of Education, Science and Technological Development of the Republic of Serbia (Project No. 172036).

Appendix A. Supplementary data

CCDC 1035721–1035722 contains the supplementary crystallographic data for $[cis,trans\text{-}\{Pt(1,3\text{-}pnd)Cl\}_2(\mu\text{-}pz)]Cl_2\cdot 2[Pt(1,3\text{-}pnd)Cl_2]\cdot 2H_2O$ and $[\{Pt(2,2\text{-}diMe\text{-}1,3\text{-}pd)Cl\}_2(\mu\text{-}pz)]Cl_2\cdot 2[Li(H_2O)_4]Cl\cdot 2H_2O$. These data can be obtained free of charge via http://www.ccdc.cam.ac.uk/conts/retrieving.html, or from the Cambridge Crystallographic Data Centre, 12 Union Road, Cambridge CB2 1EZ, UK; fax: (+44) 1223-336-033; or e-mail: deposit@ccdc.cam.ac.uk. Supplementary data associated with this article can be found, in the online version, at http://dx.doi.org/10.1016/j.poly.2016.06.011.

References

[1] D.P. Ašanin, M.D. Živković, S. Rajković, B. Warżajtis, U. Rychlewska, M.I. Djuran, Polyhedron 51 (2013) 255.
[2] S. Rajković, U. Rychlewska, B. Warżajtis, D.P. Ašanin, M.D. Živković, M.I. Djuran, Polyhedron 67 (2014) 279.
[3] S. Rajković, D.P. Ašanin, M.D. Živković, M.I. Djuran, Polyhedron 65 (2013) 42.
[4] L. Zhu, N.M. Kostić, Inorg. Chem. 31 (1992) 3994.
[5] H. Hohmann, R. van Eldik, Inorg. Chim. Acta 174 (1990) 87.
[6] N. Summa, T. Soldatović, L. Dahlenburg, Ž.D. Bugarčić, R. van Eldik, J. Biol. Inorg. Chem. 12 (2007) 461.
[7] M.D. Živković, D.P. Ašanin, S. Rajković, M.I. Djuran, Polyhedron 30 (2011) 947.
[8] S. Komeda, G.V. Kalayda, M. Lutz, A.L. Spek, Y. Yamanaka, T. Sato, M. Chikuma, J. Reedijk, J. Med. Chem. 46 (2003) 1210.
[9] L. Senerović, M.D. Živković, A. Veselinović, A. Pavić, M.I. Djuran, S. Rajković, J. Nikodinović-Runić, J. Med. Chem. 58 (2015) 1442.
[10] G. Mahal, R. van Eldik, Inorg. Chem. 24 (1985) 4165.
[11] K.J. Laidler, Chemical Kinetics, third ed., Harper & Row, New York, 1987, p. 22.
[12] CrysAlis Pro, Agilent Technologies, Yarnton, Oxfordshire, England, 2012.
[13] G.M. Sheldrick, Acta Crystallogr., Sect. A 64 (2008) 112.

[14] I.J. Bruno, J.C. Cole, P.R. Edgington, M. Kessler, C.F. Macrae, P. McCabe, J. Pearson, R. Taylor, Acta Crystallogr., Sect. B 58 (2002) 389.
[15] Stereochemical Workstation Operation Manual, Release 3.4, Siemens Analytical X-Ray Instruments Inc., Madison, WI, USA, 1989.
[16] M. Willermann, C. Mulcahy, R.K.O. Sigel, M. Morell Cerda, E. Freisinger, P.J.S. Miguel, M. Roitzsch, B. Lippert, Inorg. Chem. 45 (2006) 2093.
[17] S.U. Milinković, T.N. Parac, M.I. Djuran, N.M. Kostić, J. Chem. Soc., Dalton Trans. (1997) 2771.
[18] M.D. Živković, S. Rajković, U. Rychlewska, B. Warżajtis, M.I. Djuran, Polyhedron 26 (2007) 1541.
[19] S. Rajković, B.Đ. Glišić, M.D. Živković, M.I. Djuran, Bioorg. Chem. 37 (2009) 173.
[20] N.M. Milović, N.M. Kostić, in: A. Sigel, H. Sigel (Eds.), Metal Ions in Biological Systems, Palladium(II) and Platinum(II) Complexes as Synthetic Peptidases, vol. XXXVIII, Marcel Dekker Inc., 2001, p. 145.
[21] S. Rajković, M.D. Živković, C. Kállay, I. Sóvágó, M.I. Djuran, Dalton Trans. (2009) 8370.
[22] I.E. Burgeson, N.M. Kostić, Inorg. Chem. 30 (1991) 4299.
[23] T.N. Parac, N.M. Kostić, J. Am. Chem. Soc. 118 (1996) 51.
[24] T.N. Parac, N.M. Kostić, J. Am. Chem. Soc. 118 (1996) 5946.